Reprinted from Analytical Chemistry, 1991, 63.

Synchronous Scan Luminescence Techniques Monitoring Resonance and Nonresonance Fluorescence in Supersonic Jet Spectrometry Applied to Anthracene Derivatives

Cheng-Huang Lin, Hiroshi Fukii, Totaro Imasaka, and Nobuhiko Ishibashi*

Faculty of Engineering, Kyushu University, Hakozaki, Fukuoka 812, Japan

A supersonic jet/fluorescence spectrum is measured either by monitoring fluorescence at $\lambda_{em} = \lambda_{ex}$ (resonant synchronous scan luminescence, R-SSL) or by monitoring total fluorescence but blocking fluorescence at $\lambda_{ex} = \lambda_{em}$ (nonresonant synchronous scan luminescence, N-SSL). The R-SSL technique provides a simple spectrum and is useful for assignment of the chemical species from the database constructed by accumulating the spectral data of 0–0 transitions from the references. On the other hand the N-SSL technique offers a fingerprinting spectrum and is useful for reliable identification with the standard spectrum. A mixture sample containing anthracene, 1-, 2-, and 9-chloro-, 2- and 9-methyl-, and 2-ethylanthracene has been measured. Five compounds are readily identified by R-SSL spectrometry using a database of 0–0 transitions. However, two compounds remain unassigned. These two compounds are identified by careful assignment using the spectral data given by N-SSL spectrometry. The detection limit for anthracene achieved by N-SSL spectrometry is 7×10^{-7} M, which is 2 orders of magnitude better than the value achieved by R-SSL spectrometry. The present method is further applied to solvent-refined coal. Three components, i.e. anthracene and 1- and 2-methylanthracene, are detected in this sample.

Many polycyclic aromatic hydrocarbons (PAHs) are formed both naturally and artificially, and they are emitted into an environment. Some of them are strongly carcinogenic, and their toxicity drastically change with slight modifications in chemical structure. Therefore, a highly selective analytical method is required for assessment of pollution in the environment.

Supersonic jet expansion cools the sample molecule to several kelvin, so that it provides a sharp line structure in the ultraviolet and visible spectra (*1–3*). Supersonic jet (SSJ) spectrometry has great selectivity and allows spectrometric differentiation between molecular species with closely related structures. A combination with chromatography gives additional selectivty; even PAH isomers contained in a real sample can readily be identified (*4*). However, it is difficult to measure an excitation or multiphoton ionization spectrum during the time period that the sample passes through the detector. Therefore, the exciting wavelength should be adjusted to one of the absorption peaks for a specified component prior to the measurement. It prevents practical application of SSJ spectrometry to unknown samples.

Synchronous scan luminescence (SSL) spectrometry has been developed by Lloyd to simplify a fluorescence spectrum (*5*); the excitation and fluorescence wavelengths are synchronously scanned under the optimized separation of these wavelengths. More recently, this spectrometric technique has been applied to SSJ spectrometry (*6, 7*). It is reported to be useful for further simplification of the SSJ spectrum, giving one or two major peaks for a single component in most cases. It provides us with an effective means for analysis of a mixture sample containing many PAHs. This allows discrimination of a sample molecule from compounds with closely related structures such as isomers, which is sometimes difficult by conventional chromatography/mass spectrometry. The SSJ/SSL spectrum can be measured without prior knowledge of a sample molecule; the excitation and fluorescence wavelengths are adjusted to the same value and are scanned synchronously. Thus this method can be applied to the sample containing an unknown chemical species. This is in contrast to conventional SSL spectrometry, in which the separation between the excitation and fluorescence wavelengths should be optimized depending on the sample molecule measured.

There are, however, several disadvantages in SSJ/SSL spectrometry. The first disadvantage is a large quantity of scattered exciting light; since the monochromator wavelength is scanned by adjusting it exactly to the exciting wavelength. The second disadvantage is poor detectability, especially for a molecule whose pure electronic transition is essentially forbidden and the 0–0 transition peak is negligibly small. In this case, it is difficult even to know whether the component included is not fluorescent or if it is fluorescent but provides a negligibly small signal at the resonance transition. Moreover, only a limited number of spectral lines are observed in the SSJ/SSL spectrum, which sometimes induces an error in the assignment due to an accidental overlap of the spectral line.

In this study we develop a new SSJ/SSL spectrometric technique that has none of the limitations described above; total fluorescence is monitored by blocking fluorescence at $\lambda_{em} = \lambda_{ex}$ (nonresonant synchronous scan luminescence spectrometry, N-SSL). In contrast to conventional resonant synchronous scan luminescence spectrometry (R-SSL), this method is more sensitive and is applicable to the sample whose electronic transition is essentially forbidden but is vibrationally allowed. Furthermore, the sample molecule is more reliably assigned from a fingerprinting pattern observed. A combination of R-SSL and N-SSL (R/N-SSL), in which both spectra are shown in the same graph, provides further information about molecular structure. Therefore, this approach is versatile for reliable assignment of the chemical species in SSJ spectrometry.

We apply this R/N-SSL spectrometry to an artificial mixture containing several anthracene derivatives and also to solvent-refined coal. The chemical species are first assigned from the R-SSL spectrum with a database constructed by accumulating the spectral data of 0–0 transitions for ~320 compounds. The components are further identified from the N-SSL spectrum measured for standard chemicals. Finally, quantitative analysis is performed by N-SSL spectrometry due to its high sensitivity. The analytical advantages and limitations of R/N-SSL spectrometry are further discussed in this work.

EXPERIMENTAL SECTION

Principle. Optical configurations of R- and N-SSL spectrometries are schematically shown in Figure 1. In R-SSL spec-

* To whom correspondence should be addressed.

0003-2700/91/0363-1433$02.50/0

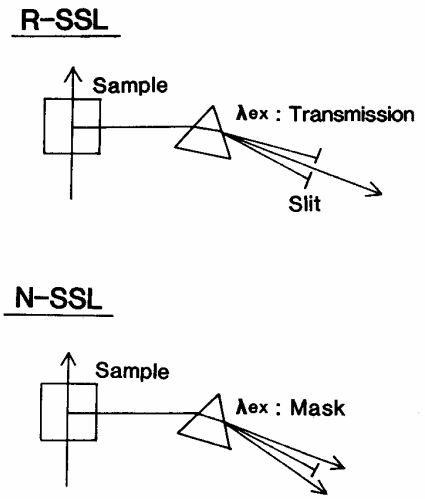

Figure 1. Optial configurations in R-SSL and N-SSL spectrometers.

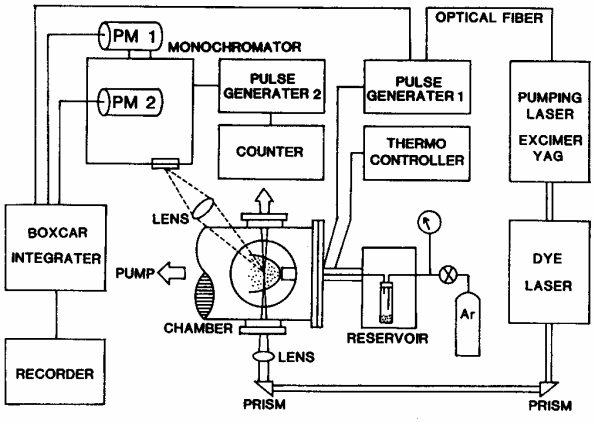

Figure 2. Experimental apparatus for measurements of excitation and R/N-SSL spectra.

trometry, photoemission at $\lambda_{em} = \lambda_{ex}$ is monitored by transmitting it through a slit of a monochromator, whose wavelength is scanned synchronously to the wavelength of the dye laser. Only resonance fluorescence is detected in this scheme. In R-SSL spectrometry, a single component gives one or two major peaks in most cases. Thus R-SSL spectrometry is useful for simplification of the spectrum. However, this is effective only for a molecule giving a strong resonance fluorescence. In contrast to R-SSL spectrometry, total fluorescence except for photoemission at $\lambda_{em} = \lambda_{ex}$ is monitored in N-SSL spectrometry by using an optical mask. This spectrometric technique is more sensitive, due to better efficiencies in fluorescence collection and in scattered-light rejection. This optical configuration has the same advantage as R-SSL spectrometry; the spectrum can be measured without prior knowledge about the spectral properties of the sample since the fluorescence spectrum is always measured by adjusting the monochromator wavelength to the dye laser wavelength.

Apparatus. The experimental apparatus constructed in this study is shown in Figure 2. An excimer-laser-pumped dye laser (Lambda Physik, EMG102MSC, FL2002) or a Nd:YAG-laser-pumped dye laser (Quantel, YG581C-20, TDL50, UVX-2, DCC-3) is used for sample excitation. The pulse width of the laser is ~10 ns, the repetition rate being 20 Hz. The sample is placed in a reservoir, whose temperature is maintained at 50–200 °C to obtain sufficient vapor pressure. For quantitative analysis, the solution sample dissolved in methanol was sprayed from a pinched restrictor continuously into a hot reservoir to vaporize (6). The sample molecule is expanded with a carrier gas of argon into a vacuum from a pulsed supersonic jet nozzle heated ~50 °C above the reservoir temperature. The vacuum chamber is evacuated by a 6-in. pump system (6). In order to obtain a sufficient cooling

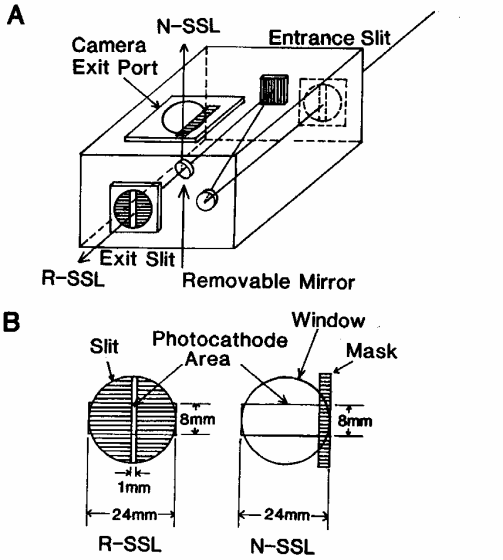

Figure 3. (A) Monochromator for recording R/N-SSL spectra. (B) Relationship between slit of monochromator and photocathode of photomultiplier.

effect, the vacuum chamber was maintained below 3 mTorr. The laser beam is focused by a quartz lens (focal length, 50 cm) into a supersonic jet 10 mm away from the nozzle. Fluorescence is collected by a quartz lens (focal length, 10 cm) onto an entrance slit of a monochromator (Jasco, CT-25CP, 2.1 nm/mm). The slit width was adjusted to 1 mm throughout this experiment. The optical configuration of the fluorescence detection port is shown in Figure 3A. The relationship between the exit port of the monochromator and the photocathode of a photomultiplier (Hamamatsu, R1477) is indicated in Figure 3B. The long axis of the photocathode is adjusted to be perpendicular to the slit of the monochromator for a wide spectral coverage in N-SSL spectrometry. This configuration decreases the sensitivity in R-SSL spectrometry, since the slit height of the monochromator (20 mm) is much larger than the photocathode width of the photomultiplier (8 mm). However, this configuration is used in this study, since it is preferential for a discussion of the sensitivities in these spectrometric methods. The direction of the last mirror is changed to up or down either for N-SSL or R-SSL spectrometry. This allows measurements of both the spectra with a minor change of the experimental conditions. For recording a N-SSL spectrum, an optical mask (width, 3 mm) is placed at $\lambda_{em} = \lambda_{ex}$. The spectral aperture is 2.1 nm for R-SSL spectrometry and 44.1 nm for N-SSL spectrometry. Thus the fluorescence collection efficiency is larger for the latter, and furthermore scattered light is completely blocked by the optical mask. So that, a better sensitivity is given for N-SSL spectrometry. The monochromator wavelength is scanned synchronously to the dye laser wavelength in both cases by a homemade pulse generator, whose pulse rate was adjusted by monitoring it with a frequency counter (NF Circuit Design Block, PC-545A). For a measurement of a conventional excitation spectrum, the monochromator wavelength was fixed to a specified fluorescence peak, and only the exciting (dye laser) wavelength was scanned. In this case the slit width was adjusted to be 1 mm (2.1 nm). The fluorescence signal is measured by a boxcar integrator (Stanford, SR250). The delay time and the gate width were changed, depending on the sample molecule measured.

Reagents. All the anthracene derivatives, biphenyl, 1-methylnaphthalene, and 2-methylnaphthalene were obtained from Tokyo Kasei, naphthalene from Kanto Chemical, and pyrene from Wako Pure Chemical. The laser dyes of BMQ, DCM, and Fluorescein 27 were purchased from Exciton. A carrier gas of argon was supplied from Iwatani.

Preparation of Real Sample. For qualitative analysis, solvent-refined coal produced and refined in Hokkaido, Japan, was placed directly in the reservoir. For quantitative analysis, solvent-refined coal (1 g) was crushed into small particles and was

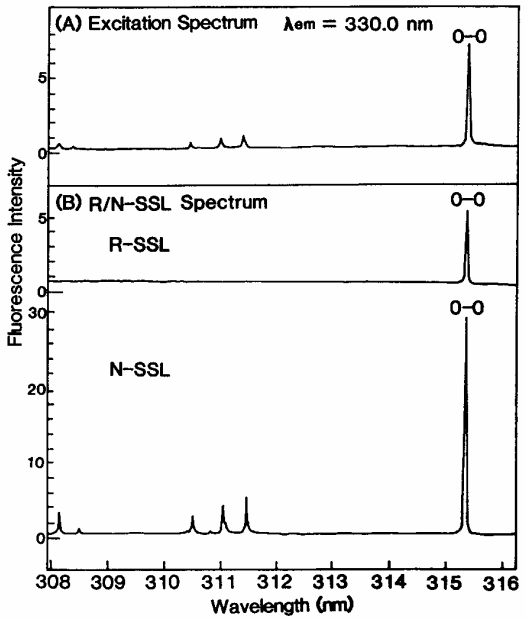

Figure 4. Supersonic jet spectra for 2-methylnaphthalene: delay time, 50 ns; gate width, 500 ns.

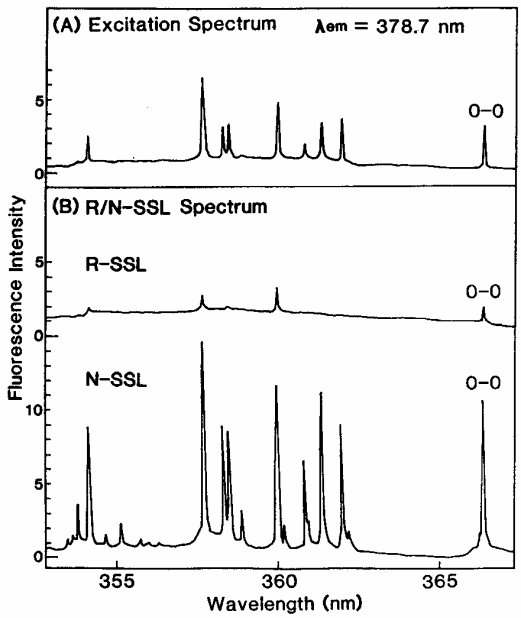

Figure 5. Supersonic jet spectra for pyrene delay time, 200 ns; gate width, 1000 ns.

dissolved in the 250-mL solvent by ultrasonic agitation during 1 h. Benzene was used as a solvent instead of methanol due to a good solubility, since only a small amount could be dissolved in methanol. The residue (0.481 g/1 g of solvent refined coal) was removed by passing the solution sample through a membrane filter (pore size, 1.0 μm).

RESULTS AND DISCUSSION

Group A (Strong 0–0 Transition). Figure 4 shows excitation and R/N-SSL spectra for 2-methylnaphthalene. In the R-SSL spectrum, a single peak is observed at the wavelength of 0–0 transition (315.40 nm). Thus R-SSL spectrometry is useful for simplification of the SSJ spectrum. In the conventional excitation spectrum, the intensity of the spectral line is proportional to the Franck-Condon factor, i.e. the overlap of the wavefunctions for the ground and excited states. This situation is identical with that in the conventional fluorescence spectrum. In the R-SSL spectrum, the spectral line appears only when the molecule is excited to a specified level and emits from this level to the ground state. Therefore, the intensity of the spectral line is proportional to the square of the Franck-Condon factor. Thus small signal peaks observed in the excitation spectrum are reduced further in the fluorescence isolation process, as designated by a "double-filter effect" (*7*). Aromatic hydrocarbons such as 9-methylanthracene, 9-chloroanthracene, and 1,2-dimethylnaphthalene give almost a single peak at 0–0 transition in the R-SSL spectrum and are grouped to this category. These compounds may readily be assigned from the database, in which the wavelengths of the 0–0 transitions have been accumulated for ~320 compounds from the reference values (*8*).

Nonresonant SSL spectrometry gives larger signal peaks, due to a better fluorescence collection efficiency. The fluorescence intensity in the N-SSL spectrum is ~5 times larger than that in the R-SSL spectrum for 2-methylnaphthalene. Furthermore, N-SSL spectrometry provides a lower background signal, since scattered exciting light is completely rejected by an optical mask. The S/N ratio is improved to 3000 for the 0–0 transition peak in N-SSL spectrometry, whereas the value is limited to 150 in R-SSL spectrometry. Thus N-SSL spectrometry is more useful in trace analysis.

Group B (Small Oscillator Strength). Supersonic jet spectra of pyrene are shown in Figure 5. The fluorescence lifetime of the S_1 state was 200–1400 ns depending on the energy level of the excited state, due to a small oscillator strength of the S_0–S_1 transition (*9*). Furthermore, the excited state has small Franck-Condon progressions, so that the fluorescence intensity is rather weak. The fluorescence intensity is much smaller than other compounds such as anthracene derivatives. In this study, the sample was heated to a higher temperature (180 °C) than the melting point (156 °C) to obtain sufficient vapor pressure, whereas the temperature was adjusted to the value slightly below the melting point for other compounds (e.g. 200 °C, mp 216 °C for anthracene). The R-SSL spectrum is more simplified than the conventional excitation spectrum, which seems to be due to mode selectivity in R-SSL spectrometry, i.e. the double-filter effect described above.

The S/N ratio is 10 in the R-SSL spectrum and 60 in the N-SSL spectrum. The scattered light is almost completely rejected even in R-SSL spectrometry by temporal discrimination. Thus the improvement of the S/N ratio by using N-SSL spectrometry is rather small in comparison with Group A (20 times).

The sample molecule may be assigned by using the database, but it should be performed carefully; several peaks are sometimes observed even in the R-SSL spectrum so that three or four peaks remain unassigned. On the other hand the N-SSL spectrum gives many spectral lines, much more than those in the conventional excitation spectrum. Then, identification of the chemical species by N-SSL spectrometry is more reliable because of the fingerprinting pattern observed.

Group C (Forbidden 0–0 Transition). Figure 6 shows excitation and R/N-SSL spectra for 1-methylnaphthalene. The S/N ratios achieved in the R- and N-SSL spectra are 360 and 2800, respectively. The weak signal peak appearing at 314.73 nm corresponds to the 0–0 transition, and a strong peak at 310.64 nm is ascribed to the $\bar{8}_0^1$ transition (*10*). Resonant SSL is useful to simplify the spectrum, even when the 0–0 transition peak is weak; small signal peaks are reduced further in the fluorescence isolation process. A similar result is observed for naphthalene. Only the wavelength of the 0–0 transition has been accumulated in the database (*8*); therefore

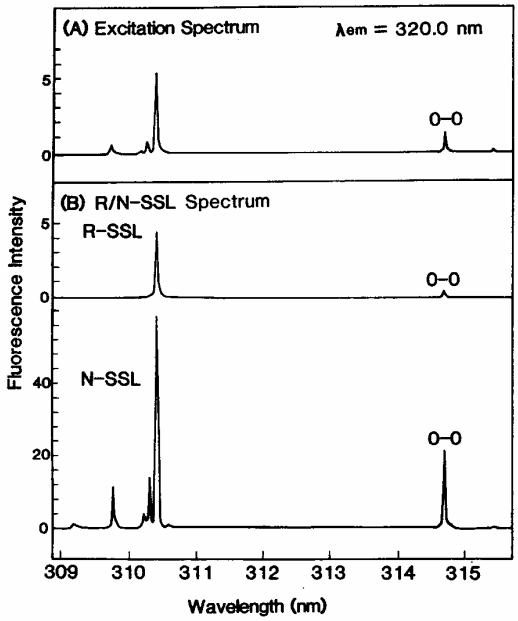

Figure 6. Supersonic jet spectra for 1-methylnaphthalene: delay time, 50 ns; gate width, 500 ns.

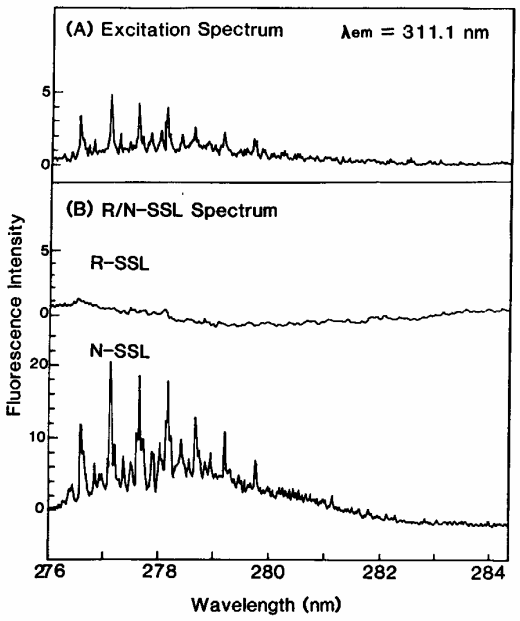

Figure 7. Supersonic jet spectra for biphenyl: delay time, 20 ns; gate time, 100 ns. Only the background signal is observed in the R-SSL spectrum.

it is difficult to identify this group of compounds using the database. So, it might be necessary to reconstruct a database to list the largest peak in the R-SSL spectrum in the future, though experimental measurements are required for many compounds.

Since the 0–0 transition peak in the R-SSL spectrum is relatively weak, this transition is implied to be electronically forbidden and vibrationally allowed. In fact, the electronic transition of naphthalene is known to be forbidden and strong vibronic peaks appear. This is due to the forbidden nature of the S_1–S_0 transition; the first and third excited singlet states have a $^1B_{3u}$ symmetry, and the S_1–S_0 transition moment disappears with configuration interaction (*11*, *12*). Thus R/N-SSL spectrometry is useful to identify whether this molecule is electronically allowed or not. It gives us additional information for assignment of the chemical species.

Group D (Twisted Molecule). Figure 7 shows excitation and R/N-SSL spectra for biphenyl. The R/N-SSL spectrum is quite different from those observed for other aromatic hydrocarbons. The 0–0 transition peak, reported to appear at 283.62 nm (*13*), is not evident in this spectrum. Biphenyl is composed of two benzene rings, which are combined with a C–C single bond. This molecule has different conformation in the ground and excited states; the electronic transition is strongly associated with a torsional motion along the C–C bond, and the equilibrium angles between two benzene rings in the excited and ground states are reported to be 44 and 0°, respectively (*13*). Therefore, the Franck-Condon factor for the 0–0 transition is negligibly small. Thus no appreciable signal appears in the R-SSL spectrum. However, when the molecule is excited to high vibrational levels in the excited state, fluorescence to high vibrational levels in the ground state is obsevable. Thus many sharp lines appear in the N-SSL spectrum.

When no signal is observed in the R-SSL spectrum, it is difficult to judge from the R-SSL spectrum whether a specified component is not included in the sample or if the fluorescence signal is negligibly small due to the small Franck-Condon factor for resonance transition. Information concerned with the energy for the 0–0 transition is difficult to be obtained even by N-SSL spectrometry, but it provides some information, at least a presence of sample. Furthermore, it is useful for identification of the sample molecule from a fingerprinting pattern as described. The S/N ratio was limited to 15 even for the largest peak in the N-SSL spectrum, due to a small Franck-Condon factor.

Analytical Procedure. Resonant and nonresonant SSL spectrometric methods have different characteristics, and the best performance is given when these spectra are presented in the same graph (R/N-SSL). The analytical procedure in this R/N-SSL spectrometry may be suggested, as follows. First, the sample may be measured by N-SSL spectrometry, owing to better sensitivity and nonspecificity. Second, R-SSL spectrometry may be applied in the same spectral region, since it greatly simplifies the spectrum. The sample component might readily be assigned from the database constructed by collecting the wavelengths of the 0–0 transition peaks or the largest peak in the R-SSL spectrum. When no experimental data are available, the database constructed by theoretical calculation of the molecular orbital might give some information in the assignment, though the error in the calculated wavelength of the 0–0 transition peak is reported to be 1–2% (*14*, *15*). Third, some information concerned with molecular structure may be obtained by comparing the R- and N-SSL spectra. For example, if the sample molecule consists of a rigid planar ring, a strong peak corresponding to the 0–0 transition might be observed in both the R- and N-SSL spectra. If no peak is observed in the R-SSL spectrum or if the 0–0 transition peak is negligibly small, the electronic transition might be forbidden or the Franck-Condon factor might be small due to a large conformational change between the excited and ground states. Fourth, the sample molecule may be further identified from a fingerprinting pattern by comparing it with the N-SSL spectra measured for the standard chemicals. Finally, quantitative analysis may be performed on the basis of N-SSL spectrometry because of its high sensitivity.

Mixture Sample. Figure 8 shows the R/N-SSL spectrum for a mixture sample containing seven anthracene derivatives. Only 10 major peaks are observed in the R-SSL spectrum. Spectral simplicity is ascribed to sufficient cooling by supersonic jet expansion and mode selectivity in R-SSL spectrometry. The signal intensity depends on the absorptivity,

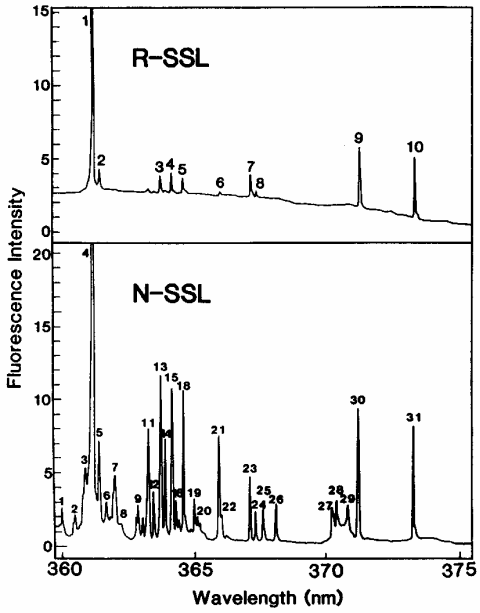

Figure 8. R/N-SSL spectrum for mixture sample containing ~10 mg of each anthracene derivative, i.e. anthracene, 1-, 2-, and 9-chloroanthracene, 2- and 9-methylanthracene, and 2-ethylanthracene.

Table I. Assignment of Signal Peaks Observed in the R- and N-SSL Spectra for the Mixture Sample[a]

experimental λ, nm				assignment		
N-SSL		R-SSL		database	R-SSL	N-SSL
1	359.98					A, 2-MA
2	360.47					2-CA, 2-MA
3	360.86					9-MA
4	361.08	1	361.08	A	A, 1-CA	A, 1-CA, 2-CA
5	361.35	2	361.35		2-CA	2-CA
6	361.63					2-MA
7	361.99					1-CA, 9-MA
8	362.17					1-CA
9	362.78					2-CA
10	363.05					1-CA
11	363.18					2-EA, 2-MA
12	363.38					2-EA
13	363.65	3	363.65		2-EA	2-CA, 2-EA
14	363.82					1-CA, 2-EA, 2-MA
15	364.07	4	364.07		2-EA	2-EA
16	364.21					2-MA
17	364.37					1-CA
18	364.50	5	364.50		2EA,2MA	2-EA, 2-MA
19	364.97			2-EA		2-EA
20	365.07			2-MA		2-MA
21	365.90	6	365.90		9-MA	9-MA
22	366.01					9-MA
23	367.09	7	367.09	2-CA	2-CA	2-CA
24	367.31	8	367.31	1-CA	1-CA	1-CA
25	367.60					9-CA
26	368.07					9-CA
27	370.15					9-CA, 9-MA
28	370.40					9-MA
29	370.78					9-MA
30	371.18	9	371.18	9-MA	9-MA	9-MA
31	373.25	10	373.25	9-CA	9-CA	9-CA

[a] Abbreviations: A, anthracene; 2-MA, 2-methylanthracene; 1-CA, 1-chloroanthracene; 9-CA, 9-chloroanthracene; 2-CA, 2-chloroanthracene; 9-MA, 9-methylanthracene; 2-EA, 2-ethylanthracene.

the fluorescence quantum yield, the Franck-Condon factor, and the partial vapor pressure of the sample at the specified temperature (200 °C). In contrast to the R-SSL spectrum, many sharp lines are observed in the N-SSL spectrum. This

Table II. Database of 0–0 Transition for Aromatic Hydrocarbons in the 360–375-nm Region

compd	0–0 transition, nm	ref
anthracene	361.08	16
1-methylanthracene	363.95	17
2-ethylanthracene	364.97[a]	6
2-methylanthracene	365.07	18
2-chloroanthracene	367.09	14
1-chloroanthracene	367.31	14
pyrene	367.44	9
phenyl nitrene	368.42	19
tropolone	370.13	20
9-(3-fluorophenyl)anthracene	370.77	18
2-phenylanthracene	370.80	18
9-(3-methylphenyl)anthracene	371.07	18
9-(4-fluorophenyl)anthracene	371.10	18
9-phenylanthracene	371.14	18
9-methylanthracene	371.18	18
9-(4-methylphenyl)anthracene	371.53	18
pyrazine	372.80	21
9-hexylanthracene	373.03	22
9-chloroanthracene	373.25	9
9-methoxyanthracene	373.40	23
9-bromoanthracene	374.20	24

[a] This signal peak is very weak in the R-SSL spectrum and is neglected in the original paper. However, this peak is rather strong in N-SSL and is tentatively assigned to the 0–0 transition in this work.

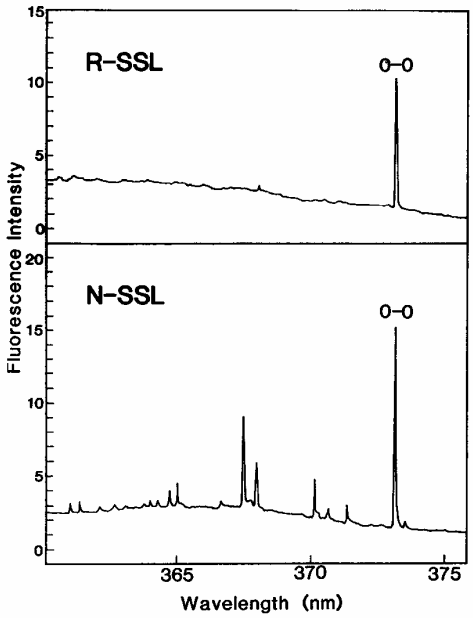

Figure 9. R/N-SSL spectrum for 9-chloroanthracene.

complicated structure is ascribed to a variety of acceptable modes in total fluorescence detection.

Assignment Using Database. The second column of Table I indicates the wavelengths of the peaks observed in the N-SSL spectrum for a mixture sample containing seven PAHs. The peaks observed in the R-SSL spectrum are shown in the fourth column. A part of the database obtained by accumulating the wavelength of the 0–0 transition from references is shown as Table II. Five peaks observed in the R-SSL spectrum, i.e. 1, 7–10, are readily assigned to the 0–0 transitions for five anthracene derivatives from the database. The other five peaks, i.e. 2–6, are due to resonance fluorescence to/from high vibrational levels in the excited stae, and then they are not assigned from the database. The remaining two compounds, i.e. 2-ethylanthracene and 2-methylanthracene,

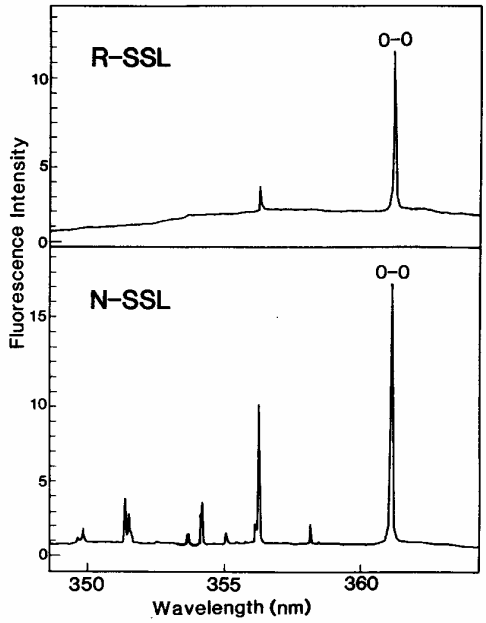

Figure 10. R/N-SSL spectrum for anthracene.

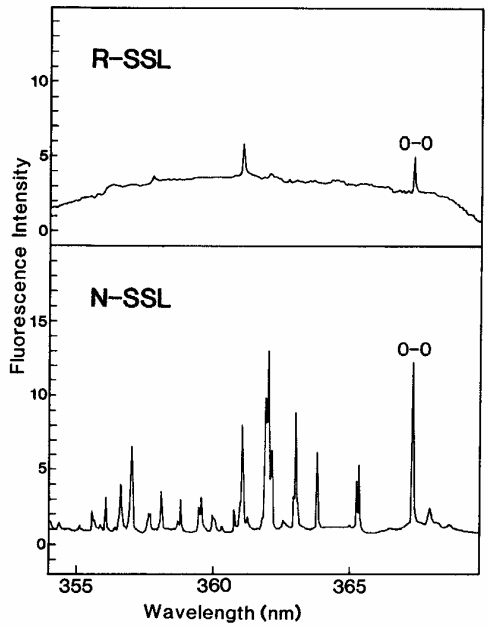

Figure 12. R/N-SSL spectrum for 1-chloroanthracene.

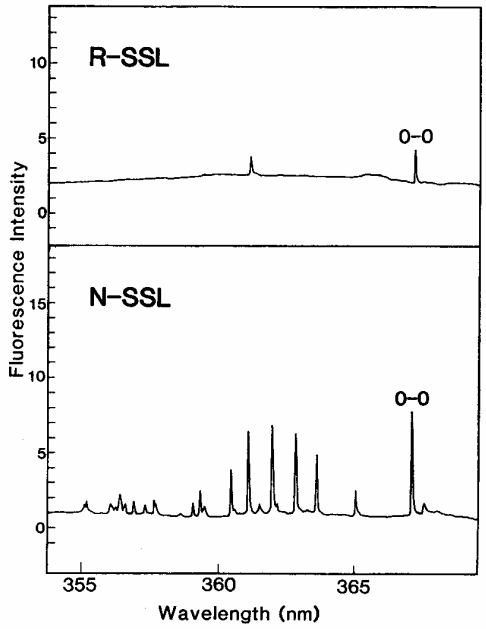

Figure 11. R/N-SSL spectrum for 2-chloroanthracene.

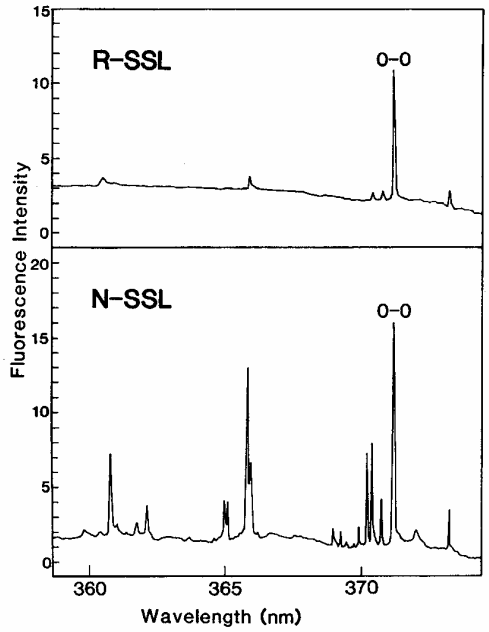

Figure 13. R/N-SSL spectrum for 9-methylanthracene.

are assigned by using the database from the spectral data given by N-SSL spectrometry. These results are summarized in the fifth column of Table I.

Identification with a Standard Spectrum. As shown in Figure 9, only a single peak is observed for 9-chloroanthracene in the R-SSL spectrum (group A). On the other hand, two major peaks are observed for anthracene and 2-chloroanthracene (similar to group B), as shown in Figures 10 and 11. Weaker signal peaks are attributed to resonance fluorescence to/from high vibrational levels in the excited state. Thus peak 2 and a part of peak 1 are attributed to 2-chloroanthracene and 1-chloroanthracene, respectively. This situation is similar to 1-chloroanthracene, as shown in Figure 12; a weak signal peak at 361.08 nm may be possible to assign to the 0–0 transition for anthracene, included as an impurity in the reagent, but the peak observed at 356.03 nm in the spectrum for anthracene is not evident so that this peak is tentatively assigned to 1-chloroanthracene. Peak 6 is also attributed to 9-methylanthracene from the spectrum shown in Figure 13. The R/N-SSL spectra are very complicated for 2-methylanthracene and 2-ethylanthracene (similar to group D), as shown in Figures 14 and 15. This is ascribed to torsional motion with a small vibrational energy or internal rotation giving many isomers along the axis of a C–C single bond between the aromatic ring and the methyl or ethyl group. Thus small peaks 3 and 4 are tentatively assigned to 2-ethylanthracene, and peak 5, to 2-ethylanthracene and 2-methylanthracene (accidental spectral overlap). The results are summarized in the sixth column of Table I.

The above assignments are further confirmed by the standard N-SSL spectra. Possible candidates of the peaks are indicated in the last column of Table I. The assignments

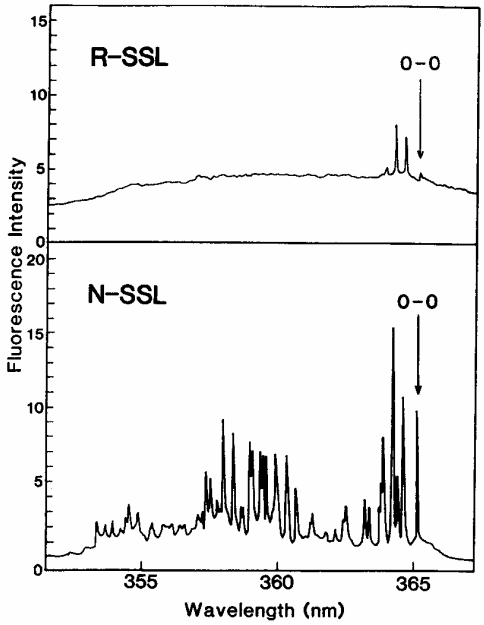

Figure 14. R/N-SSL spectrum for 2-methylanthracene.

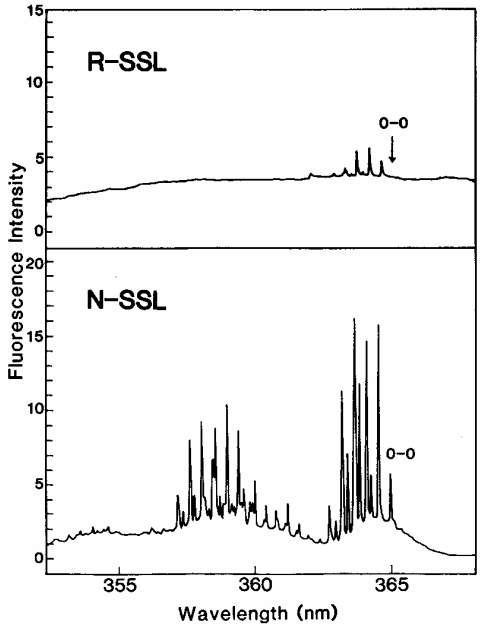

Figure 15. R/N-SSL spectrum for 2-ethylanthracene.

from the R-SSL spectra are readily confirmed. Since there are many spectral lines in the N-SSL spectrum, molecular species are more reliably identified from the fingerprinting pattern observed. However, a few candidates are given for a single peak, and therefore this method is useful only for confirmation of the assignment; it seems to be difficult to assign the chemical species only from the data obtained by N-SSL spectrometry, since it is so complicated, especially in multicomponent analysis.

Detection Limit. A R-SSL spectrum was measured by introducing the solution sample into a hot reservoir to vaporize anthracene continuously for quantitative analysis. The analytical curve was constructed in the 0–10^{-3} M range. The S/N ratio was 3 for the sample measured at a concentration of 1×10^{-4} M. The detection limit is similar to the previous value obtained for anthracene (7×10^{-5} M, $S/N = 3$) by R-SSL spectrometry (*6*). A similar analytical curve was constructed by using N-SSL spectrometry in the 0–10^{-3} M range, and the detection limit was 7×10^{-7} M. Thus the sensitivity of N-SSL spectrometry is about 2 orders of magnitude better than that of R-SSL spectrometry. It is noted that this detection limit is several times better than that of conventional fluorescence spectrometry monitoring a specific vibrational band (3×10^{-6} M) (*6*). Better sensitivity is ascribed to a higher efficiency in fluorescence collection, since total fluorescence ($\lambda_{em} \neq \lambda_{ex}$, bandpass 44.1 nm) is collected in N-SSL spectrometry.

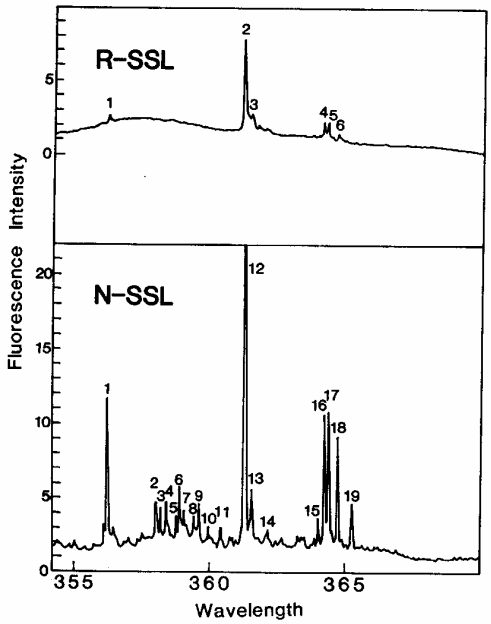

Figure 16. R/N-SSL spectrum for solvent-refined coal.

Table III. Assignment of Signal Peaks Observed in R- and N-SSL Spectra for Solvent-Refined Coal[a]

experimental λ, nm				assignment		
N-SSL		R-SSL		database	R-SSL	N-SSL
1	356.03	1	356.03		A	A
2	357.80					2-MA
3	357.98					A
4	358.17					2-MA
5	358.56					2-MA
6	358.67					?
7	358.83					2-MA
8	359.16					?
9	359.37					?
10	359.76					2-MA
11	360.20					2-MA
12	361.08	2	361.08	A	A	A
13	361.29	3	361.29		?	?
14	361.90					?
15	363.18					2-MA
16	363.95	4	363.95	1-MA	1-MA	1-MA
17	364.07	5	364.07		2-MA	2-MA
18	364.50	6	364.50		2-MA	2-MA
19	365.07			2-MA		2-MA

[a] Abbreviations: A, anthracene; 2-MA, 2-methylanthracene; 1-MA, 1-methylanthracene; ?, unassigned.

Real Sample. Figure 16 shows the R/N-SSL spectrum for solvent-refined coal. The experimental results are summarized in the second and fourth columns of Table III. Apparently, peak 2 in the R-SSL spectrum is assigned to the 0–0 transition for anthracene from the database. Of particular interest is peak 4, which can be assigned to 1-methylanthracene from the database, though this compound is not commercially

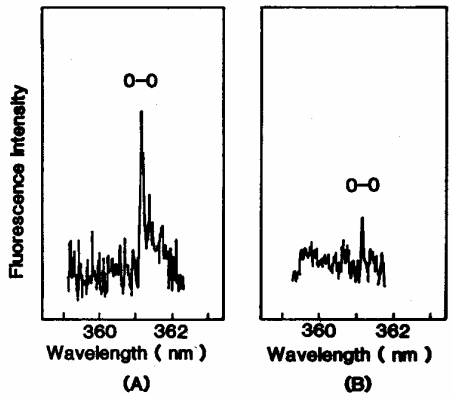

Figure 17. N-SSL spectrum for (A) anthracene (10^{-5} M) and (B) solvent-refined coal. The samples are dissolved in benzene.

available and has not been measured in this study. From the standard spectrum, peak 1 is assigned to resonance fluorescence from the 12^1 level of anthracene. Peaks 5 and 6 are assigned to 2-methylanthracene from the standard R-SSL spectrum. Presences of anthracene and 2-methylanthracene are confirmed further from the N-SSL spectra for the standards. However, several unassigned peaks remain in the R-SSL and N-SSL spectra. They might possibly originate from other anthracene derivatives. Further investigation may be necessary for the assignments, due to lack of spectral data and of the standard chemical.

Quantitative analysis is perfomed for solvent-refined coal by using N-SSL spectrometry, since it is more sensitive than both R-SSL and conventional fluorescence spectrometries. Figure 17A,B shows the N-SSL spectra for anthracene (1×10^{-5} M) and solvent-refined coal in benzene, respectively. In order to avoid errors induced by nonlinearity of signal response, the standard spectrum was measured at anthracene concentrations similar to that of the real sample. The spectral peak for standard anthracene is slightly shaded to longer wavelengths, which is probably due to formation of van der Waals complexes with benzene. No such spectral shade was observed for anthracene dissolved in methanol. This is considered to be due to a strong interaction between π electrons in anthracene and benzene. The signal intensity of the 0–0 transition peak for anthracene in solvent-refined coal is quite small but is evident; the measurement was repeated, and the signal was confirmed to be reproducible. From the intensity ratio of the signal peaks in Figure 17A,B, the concentration of anthracene is determined to be 3×10^{-6} M. The content of anthracne in solvent-refined coal was calculated to be 100 ppm (10^{-4} g of anthracene/1 g of solvent refined coal).

Advantage and Limitation. Resonant SSL spectrometry gives a simple spectrum, and the major peak is mostly assigned from the database of 0–0 transitions, especially for a rigid molecule; there is little configuration change, and the Franck-Condon factor is the largest for the 0–0 transition. This approach is simple and straightforward, since the database is constructed by accumulating the reference data without any experimental work. However, the assignment only from this database is sometimes imperfect, as experienced in this work, for a molecule giving a weak 0–0 transition peak. In this case several components remain unassigned. Moreover, many peaks are observed, especially for a molecule with a low torsional vibrational mode and for a molecule consisting of rotational isomers. In this case several peaks remain unassigned. Thus there are some limitations in assignment of chemical species by using the database of 0–0 transition alone. The database constructed by accumulating the major peaks in the R-SSL spectrum will be more useful, though it requires a lot of experimental work.

There are a limited number of spectral peaks in the R-SSL spectrum, i.e. one or two major peaks for a single component. However, superposition of the signal peak is sometimes unavoidable, as in the cases of anthracene and 1-chloroanthracene or 2-methylanthracene and 2-ethylanthracene. Then, efficient sample cooling and accurate wavelength calibration are essential for reliable assignment. The sensitivity of R-SSL spectrometry is rather poor, which is mainly due to background increase by scattered light of the dye laser. A time-resolved fluorescence spectrometer with a subnanosecond resolution may be useful for background discrimination in determination of anthracene derivatives having rather short fluorescence lifetimes (several nanoseconds).

The N-SSL spectrum consists of more than 30 major peaks for a mixture sample containing seven anthracene derivatives. This approach is more useful for reliable identification. However, the construction of the database is more difficult in N-SSL spectrometry, since more than 10 peaks appear from a single component. Therefore, many spectral parameters should be accumulated for construction of a database. Filing the spectral data and searching the candidates by a computer will be necessary for more reliable assignment in the future.

A combination of R- and N-SSL spectrometries proides us with a sensitive and selective analytical means, due to the spectral simplicity of R-SSL spectrometry and to the high sensitivity of N-SSL spectrometry. This spectrometric method might be applicable not only to anthracene derivatives in solvent-refined coal but also to other PAHs in the environment such as benzo[*a*]pyrene in airborne particulates. Thus R/N-SSL spectrometry may have wide application fields and is useful especially in determination of the sample containing many PAH molecules with closely related structures.

Registry No. Anthracene, 120-12-7; 1-chloroanthracene, 4985-70-0; 2-chloroanthracene, 17135-78-3; 9-chloroanthracene, 716-53-0; 2-methylanthracene, 613-12-7; 9-methylanthracene, 52251-71-5; 1-methylanthracene, 610-48-0.

LITERATURE CITED

(1) Hayes, J. M.; Small, G. J. *Anal. Chem.* **1983**, *55*, 565A.
(2) Johnston, M. V. *Tr AC, Trends Anal. Chem.* **1984**, *3*, 58.
(3) Lubman, D. M. *Anal. Chem.* **1987**, *59*, 31A.
(4) Imasaka, T.; Ishibashi, N. *Prog. Quantum Electron.* **1990**, *14*, 131 (Section 7.5.5, p 222).
(5) Lloyd, J. B. F. *Nature (London)* **1971**, *231*, 64.
(6) Imasaka, T.; Tsukamoto, A.; Ishibashi, N. *Anal. Chem.* **1988**, *60*, 1362.
(7) Imasaka, T.; Maeno, I.; Ishibashi, N. *Analyst* **1990**, *115*, 73.
(8) Ishibashi, N.; Imasaka, T. Report For Grant-in-Aid for Scientific Research from the Ministry of Education of Japan; Project No. 01470065.
(9) Mangle, E. A.; Topp, M. R. *J. Phys. Chem.* **1986**, *90*, 802.
(10) Warren, J. A.; Hayes, J. M.; Small, G. J. *J. Chem. Phys.* **1984**, *80*, 1786.
(11) Dewar, M. J. S.; Longuet-Higgins, H. C. *Proc. Phys. Soc. London, Sect. A* **1954**, *67*, 795.
(12) Jacobson, B. A.; Guest, J. A.; Novak, F. A.; Rice, S. A. *J. Chem. Phys.* **1987**, *87*, 269.
(13) Im, H. S.; Bernstein, E. R. *J. Chem. Phys.* **1988**, *88*, 7337.
(14) Imasaka, T.; Ishibashi, N. *Spectrochim. Acta* **1988**, *43B*, 661.
(15) Imasaka, T.; Sakaki, K.; Ishibashi, N. *Chemom. Intell. Lab. Syst.* **1989**, *6*, 281.
(16) Lambert, W. R.; Felker, P. M.; Syage, J. A.; Zewail, A. H. *J. Chem. Phys.* **1984**, *81*, 2195.
(17) Pepich, B. V.; Callis, J. B.; Burns, D. H.; Gouterman, M. *Anal. Chem.* **1986**, *58*, 2825.
(18) Werest, D. W.; Brearley, A. M.; Gentry, W. R.; Barbara, P. F. *J. Am. Chem. Soc.* **1987**, *109*, 32.
(19) Ozawa, K.; Ishida, T.; Fuke, K.; Kaya, K. *Chem. Phys. Lett.* **1988**, *150*, 249.
(20) Redington, R. L. *J. Chem. Phys.* **1988**, *88*, 627.
(21) Pennor, A.; Amirav, *J. Phys. Chem.* **1988**, *92*, 5079.
(22) Syage, J. A.; Gelker, P. M.; Semmes, D. H.; Adel, F. A.; Zewail, A. H. *J. Chem. Phys.* **1985**, *82*, 2896.
(23) Hirayama, S. *Chem. Phys. Lett.* **1988**, *153*, 112.
(24) Amirav, A.; Horwitz, C.; Jortner, J. *J. Chem. Phys.* **1988**, *88*, 2092.

RECEIVED for review December 17, 1990. Accepted April 1, 1991. This research is supported by Grants-in-Aid for Scientific Research from the Ministry of Education of Japan and by the Kurata Foundation.